[1.]Nebojša RADIĆ, [2.]Dejan JEREMIĆ

INVESTIGATION OF VIBRATION RESPONSE OF ORTHOTROPIC DOUBLE-NANOPLATE SYSTEM SUBJECTED TO INITIAL IN-PLANE PRELOAD

[1-2.]University of East Sarajevo, Faculty of Mechanical Engineering, East Sarajevo, BOSNIA & HERZEGOVINA

Abstract: Analytical methods are employed and explicit solutions for vibrational frequency are obtained for orthotropic double-nanoplate system subjected to an in-plane magnetic field for various boundary conditions. The nonlocal governing equations of motion are derived via Hamilton's principle with the consideration the Eringen's differential nonlocal elastic law. Effects of initial preload (compression and tension), magnetic field strength, size of nanoplate, and boundary conditions on vibrational frequency are presented.
Keywords: graphene, initial preload, magnetic field, nanoplate, nonlocal elasticity, vibration

1. INTRODUCTION

Carbon nanotube (CNT) and graphene sheet (GS) have a great perspective to be applied in medicine, astronautics and energy storage systems. For a successful application of GS as a nanostructural component and a nanomaterial it is very important to know its vibrational behaviour. Experimental and molecular dynamic simulation (MD simulation) show that in nanostructural elements with very small dimensions their mechanical properties and behaviour change when these dimensions become very small. Due to very small dimensions of nanoplates, it is necessary to take into account the influence of atomic forces to their mechanical behaviour. The application of MD simulation is too complex and expensive, especially in the case of more complex nanostructures with a greater number of atoms. Because of that, a few classical continuum theories have been developed in which the small-scale size effect has been incorporated into constitutive equations and governing equations of motion/equilibrium. There belong the nonlocal elasticity theory [1-4], strain gradient theory [5,6] and couple stress theory [7,8]. The effect of in-plane preload on vibrations of nanoplate via nonlocal elasticity was investigated by Murmu and Pradhan [9]. Kiani [10] applied the nonlocal shear deformation theory to investigate the vibration of double-walled carbon nanotubes on elastic foundation subjected to axial preload. Mohammadi et al. [11] investigated the free vibration behaviour of circular graphene sheet under in-plane preload using nonlocal continuum theory. In recent time, double-layered nanoplate structures have been in the focus of research more. Radić and Jeremić [12] researched the nonlocal vibration and buckling of orthotropic double-layered graphene sheets with different boundary conditions subjected to hygrothermal loading using nonlocal elasticity theory and Galerkin's method.

When a nanostructure is exposed to the activity of magnetic field, then, as the consequence of the activity, Lorentz's forces occur, which are the body forces and act to every elementary particle of that structure. In the absence of experimental research on the influence of Lorentz's forces to the vibration and buckling behaviour of nanoplates, a great significance is given to the theoretical research based on Maxwell's equations. Güven [13] studied the effects of longitudinal magnetic field and initial stress on the transverse vibration of single-walled carbon nanotubes. Murmu et al. [14] examined vibration behaviour of double-walled carbon nanotubes subjected to a longitudinal magnetic field using a nonlocal Euler-Bernoulli beam theory. Kiani [15] investigated the vibration and instability of a single-walled carbon nanotube in a three-dimensional magnetic field using nonlocal Rayleigh beam theory. Transverse vibration behaviour of embedded single-layer graphene sheets exposed to in-plane magnetic field with simply supported boundary conditions is analysed by Murmu et al. [16]. Kiani [17] presented free vibration behaviour of single-layer nanoplates subjected to in-plane magnetic field with simply supported boundary conditions using nonlocal shear deformable plate theories. Vibration behaviour of double bonded orthotropic graphene sheets subjected to 2D magnetic field and biaxial in-plane preload using differential quadrature method was investigated by Ghorbanpour Arani et al [18]. Karličić et al. [19] investigated the nonlocal vibration of multi-nanoplate system embedded in viscoelastic medium under in-plane magnetic field. Transverse vibration analysis of the orthotropic DLGSs subjected to in-plane magnetic and initial in-plane preload with various boundary conditions has not been covered using nonlocal continuum mechanics until now.

In the present paper, using differential nonlocal elastic law we study the influence of a unidirectional in-plane magnetic field and initial in-plane preload on the vibration behaviour of DLGS. The governing equations of motion are derived based on new first-order shear deformation theory (NFSDT), Eringen's differential nonlocal elastic law and the Hamilton's principle. Analytical solution for frequency is based on functions which satisfy different boundary conditions.

2. PROBLEM FORMULATION

DLGS which consists of two layers of graphene sheets (GS_1 and GS_2), with length a, width b and thickness h embedded in Pasternak foundation subjected to in-plane magnetic field H_x has been illustrated in Figure 1.

GS_1 and GS_2 are in the interaction by van der Waals (vdW) interaction forces shown by a set of springs with modulus k_0. Two sheets are surrounded by an external Pasternak elastic medium, where k_w and k_G are Winkler modulus parameter and shear modulus parameter respectively. As depicted N_{xx}^0 and N_{yy}^0 denote two uniform preload forces in the *x* and *y* directions. The material characteristics used for both graphene sheets are identical.

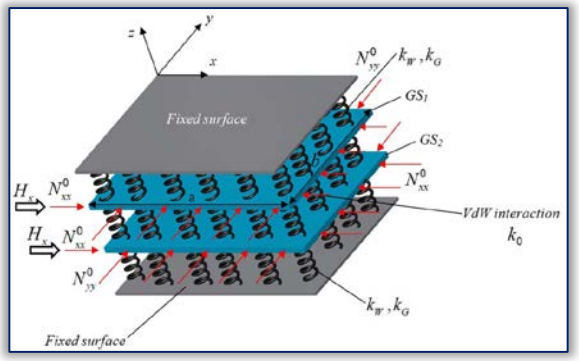

Figure 1. Geometry, coordinate system and loading for orthotropic double-layered graphene sheet

2. THE NEW FIRST-ORDER SHEAR DEFORMATION THEORY (NFSDT)

According to the new first-order shear deformation theory, the displacement field of the graphene sheet is expressed by

$$\begin{aligned} u_x(x,y,z) &= u(x,y) - z\frac{\partial \phi}{\partial x} \\ u_y(x,y,z) &= v(x,y) - z\frac{\partial \phi}{\partial y} \\ u_z(x,y,z) &= w(x,y) \end{aligned} \tag{1}$$

where u and v are the displacement of mid-plane along *x*- and *y*-axis respectively, w is transverse displacement of a point on the mid-plane of the graphene sheet, and ϕ is rotation parameter.

Nonzero strains of the NFSDT model are expressed as

$$\begin{Bmatrix} \varepsilon_{xx} \\ \varepsilon_{yy} \\ \varepsilon_{xy} \end{Bmatrix} = \begin{Bmatrix} \dfrac{\partial u}{\partial x} \\ \dfrac{\partial v}{\partial y} \\ \dfrac{\partial u}{\partial y} + \dfrac{\partial v}{\partial x} \end{Bmatrix} - z \begin{Bmatrix} \dfrac{\partial^2 \theta}{\partial x^2} \\ \dfrac{\partial^2 \theta}{\partial y^2} \\ 2\dfrac{\partial^2 \theta}{\partial x \partial y} \end{Bmatrix}, \begin{Bmatrix} \varepsilon_{yz} \\ \varepsilon_{xz} \end{Bmatrix} = \begin{Bmatrix} \dfrac{\partial w}{\partial y} - \dfrac{\partial \theta}{\partial y} \\ \dfrac{\partial w}{\partial x} - \dfrac{\partial \theta}{\partial x} \end{Bmatrix} \tag{2}$$

3. NONLOCAL GOVERNING EQUATIONS OF MOTION

In the present paper, we consider a uniaxial magnetic field. Therefore, the effective Lorenz forces in the direction of z axis can be written as [20].

$$F_z = \int_{-h/2}^{h/2} f_z dz = \eta h H_x^2 \left(\frac{\partial^2 w}{\partial x^2} - \frac{\partial^2 \theta}{\partial y^2} \right) \tag{3}$$

In this study only the transverse vibrations of the DLGS are significant.

For this case, the equations that correspond to the in-plane displacements $(\delta u_1, \delta v_1)$ are not coupled with the equations that correspond to the displacements due to bending. If we apply the operator $\Re = 1 - (e_0 \ell)^2 \nabla^2$ equations of motion can be expressed via the displacement (w_1, ϕ_1)

$$\begin{aligned} &H_{55}\left(\frac{\partial^2 w_1}{\partial x^2} - \frac{\partial^2 \phi_1}{\partial x^2}\right) + H_{44}\left(\frac{\partial^2 w_1}{\partial y^2} - \frac{\partial^2 \phi_1}{\partial y^2}\right) - k_w w_1 + k_G\left(\frac{\partial^2 w_1}{\partial x^2} + \frac{\partial^2 w_1}{\partial y^2}\right) - k_0(w_1 - w_2) - \\ &- N_{xx}^0 \frac{\partial^2 w_1}{\partial x^2} - N_{yy}^0 \frac{\partial^2 w_1}{\partial y^2} + \eta h H_x^2 \left(\frac{\partial^2 w_1}{\partial x^2} - \frac{\partial^2 \phi_1}{\partial y^2}\right) - \\ &- (e_0\ell)^2 \left[-k_w\left(\frac{\partial^2 w_1}{\partial x^2} + \frac{\partial^2 w_1}{\partial y^2}\right) + k_G\left(\frac{\partial^4 w_1}{\partial x^4} + 2\frac{\partial^4 w_1}{\partial x^2 \partial y^2} + \frac{\partial^4 w_1}{\partial y^4}\right)\right] \\ &+ (e_0\ell)^2 k_0\left(\frac{\partial^2 w_1}{\partial x^2} + \frac{\partial^2 w_1}{\partial y^2} - \frac{\partial^2 w_2}{\partial x^2} - \frac{\partial^2 w_2}{\partial y^2}\right) + (e_0\ell)^2 N_{xx}^0\left(\frac{\partial^4 w_1}{\partial x^4} + \frac{\partial^4 w_1}{\partial x^2 \partial y^2}\right) \\ &+ (e_0\ell)^2 N_{yy}^0\left(\frac{\partial^4 w_1}{\partial y^4} + \frac{\partial^4 w_1}{\partial x^2 \partial y^2}\right) - (e_0\ell)^2 \eta h H_x^2 \left[\left(\frac{\partial^4 w_1}{\partial x^4} + \frac{\partial^4 w_1}{\partial x^2 \partial y^2}\right) - \left(\frac{\partial^4 \phi_1}{\partial y^4} + \frac{\partial^4 \phi_1}{\partial x^2 \partial y^2}\right)\right] = \\ &= \rho h \ddot{w}_1 - (e_0\ell)^2 \rho h\left(\frac{\partial^2 \ddot{w}_1}{\partial x^2} + \frac{\partial^2 \ddot{w}_1}{\partial y^2}\right) \end{aligned} \tag{4}$$

$$D_{11}\frac{\partial^4\phi_1}{\partial x^4}+2\left(D_{12}+2D_{66}\right)\frac{\partial^4\phi_1}{\partial x^2\partial y^2}+D_{22}\frac{\partial^4\phi_1}{\partial y^4}+H_{55}\left(\frac{\partial^2 w_1}{\partial x^2}-\frac{\partial^2\phi_1}{\partial x^2}\right)+$$
$$+H_{44}\left(\frac{\partial^2 w_1}{\partial y^2}-\frac{\partial^2\phi_1}{\partial y^2}\right)=\frac{\rho h^3}{12}\left(\frac{\partial^2\ddot{\phi}_1}{\partial x^2}+\frac{\partial^2\ddot{\phi}_1}{\partial y^2}\right)-\left(e_0\ell\right)^2\frac{\rho h^3}{12}\left(\frac{\partial^4\ddot{\phi}_1}{\partial x^4}+2\frac{\partial^4\ddot{\phi}_1}{\partial x^2\partial y^2}+\frac{\partial^4\ddot{\phi}_1}{\partial y^4}\right) \quad (5)$$

Eqs. (4) and (5) are related to GS_1. In the same way the equations of motion for GS_2 are obtained.

$$H_{55}\left(\frac{\partial^2 w_2}{\partial x^2}-\frac{\partial^2\phi_2}{\partial x^2}\right)+H_{44}\left(\frac{\partial^2 w_2}{\partial y^2}-\frac{\partial^2\phi_2}{\partial y^2}\right)-k_W w_2+k_G\left(\frac{\partial^2 w_2}{\partial x^2}+\frac{\partial^2 w_2}{\partial y^2}\right)+k_0\left(w_1-w_2\right)+$$
$$-N_{xx}^0\frac{\partial^2 w_2}{\partial x^2}-N_{yy}^0\frac{\partial^2 w_2}{\partial y^2}+\eta hH_x^2\left(\frac{\partial^2 w_2}{\partial x^2}-\frac{\partial^2\phi_2}{\partial y^2}\right)-$$
$$-\left(e_0\ell\right)^2\left[-k_W\left(\frac{\partial^2 w_2}{\partial x^2}+\frac{\partial^2 w_2}{\partial y^2}\right)+k_G\left(\frac{\partial^4 w_2}{\partial x^4}+2\frac{\partial^4 w_2}{\partial x^2\partial y^2}+\frac{\partial^4 w_2}{\partial y^4}\right)\right] \quad (6)$$
$$-\left(e_0\ell\right)^2 k_0\left(\frac{\partial^2 w_1}{\partial x^2}+\frac{\partial^2 w_1}{\partial y^2}-\frac{\partial^2 w_2}{\partial x^2}-\frac{\partial^2 w_2}{\partial y^2}\right)+\left(e_0\ell\right)^2 N_{xx}^0\left(\frac{\partial^4 w_2}{\partial x^4}+\frac{\partial^4 w_2}{\partial x^2\partial y^2}\right)$$
$$+\left(e_0\ell\right)^2 N_{yy}^0\left(\frac{\partial^4 w_2}{\partial y^4}+\frac{\partial^4 w_2}{\partial x^2\partial y^2}\right)-\left(e_0\ell\right)\eta hH_x^2\left[\left(\frac{\partial^4 w_2}{\partial x^4}+\frac{\partial^4 w_2}{\partial x^2\partial y^2}\right)-\left(\frac{\partial^4\phi_2}{\partial y^4}+\frac{\partial^4\phi_2}{\partial x^2\partial y^2}\right)\right]=$$
$$=\rho h\ddot{w}_2-\left(e_0\ell\right)^2\rho h\left(\frac{\partial^2\ddot{w}_2}{\partial x^2}+\frac{\partial^2\ddot{w}_2}{\partial y^2}\right)$$

$$D_{11}\frac{\partial^4\phi_2}{\partial x^4}+2\left(D_{12}+2D_{66}\right)\frac{\partial^4\phi_2}{\partial x^2\partial y^2}+D_{22}\frac{\partial^4\phi_2}{\partial y^4}+H_{55}\left(\frac{\partial^2 w_2}{\partial x^2}-\frac{\partial^2\phi_2}{\partial x^2}\right)+$$
$$+H_{44}\left(\frac{\partial^2 w_2}{\partial y^2}-\frac{\partial^2\phi_2}{\partial y^2}\right)=\frac{\rho h^3}{12}\left(\frac{\partial^2\ddot{\phi}_2}{\partial x^2}+\frac{\partial^2\ddot{\phi}_2}{\partial y^2}\right)- \quad (7)$$
$$-\left(e_0\ell\right)^2\frac{\rho h^3}{12}\left(\frac{\partial^4\ddot{\phi}_2}{\partial x^4}+2\frac{\partial^4\ddot{\phi}_2}{\partial x^2\partial y^2}+\frac{\partial^4\ddot{\phi}_2}{\partial y^4}\right)$$

The equations (4-7) present the equations of motion for orthotropic DLGSs.

4. SOLUTION BY GALERKIN'S METHOD

In this section, the equations of motion (4-7) are solved analytically using Galerkin's method to obtain the vibrational frequencies of the DLGSs subjected to in-plane preload. Before solving the equations of motion, the boundary conditions should be defined. In this study the graphene sheet is assumed to have simply supported (S), clamped (C) edges or have combinations of them. These boundary conditions are given as follows [12].

Simply supported (S):

$$u_i=\frac{\partial\phi_i}{\partial y}=w_i=M_{xxi}=0,\quad \text{at } x=0,\mathrm{a}$$
$$v_i=\frac{\partial\phi_i}{\partial x}=w_i=M_{yyi}=0,\quad \text{at } y=0,b;\ \ i=1,2 \quad (8)$$

Clamped (C):

$$u_i=\frac{\partial\phi_i}{\partial x}=\frac{\partial\phi_i}{\partial y}=w_i=0,\quad \text{at } x=0,\mathrm{a}$$
$$v_i=\frac{\partial\phi_i}{\partial x}=\frac{\partial\phi_i}{\partial y}=w_i=0,\quad \text{at } y=0,b;\ \ i=1,2 \quad (9)$$

The analytical solutions for the vibrational frequency are obtained for two characteristics of the vibration cases.

— Out-of-phase vibration

In this case, two graphene sheets vibration asynchronously and it means that there is a relative displacement between them $\left(w_1\neq w_2\right)$. The equation (10) represent the value for the vibrational frequency for out-of-phase vibration

$$\omega_{out}=\sqrt{\frac{-A_4+\sqrt{A_4^2-4A_1A_5}}{2A_1}} \quad (10)$$

$$A_1=\frac{\rho^2h^4}{12}\left(\gamma_4-\mu^2\delta_1\right)\left(\delta_1-\mu^2\delta_2\right)$$
$$A_4=\rho h\left(\gamma_4-\mu^2\delta_1\right)\left(B_3-B_2\right)+\frac{\rho h^3}{12}\left(\delta_1-\mu^2\delta_2\right)\left[P_3+2k_0\left(\mu^2\delta_1-\gamma_4\right)\right]$$
$$A_5=P_3\left(B_3-B_2\right)-B_2\left(B_4-B_2\right)+2k_0\left(\mu^2\delta_1-\gamma_4\right)\left(B_3-B_2\right)$$
$$P_1=k_w(\mu^2\delta_1-\gamma_4)+k_G(\delta_1-\mu^2\delta_2)+\eta hH_x^2\left[\gamma_1-\mu^2(\gamma_3+\gamma_6)\right]$$

where:

$$\begin{aligned}
\delta_1 &= \gamma_1 + \gamma_2 \\
\delta_2 &= \gamma_3 + 2\gamma_6 + \gamma_5 \\
B_2 &= H_{55}\gamma_1 + H_{44}\gamma_2 \\
B_3 &= D_{11}\gamma_3 + 2(D_{12} + 2D_{66})\gamma_6 + D_{22}\gamma_5 \\
B_4 &= \eta h H_x^2 \left[\mu^2 (\gamma_5 + \gamma_6) - \gamma_2 \right] \\
P_3 &= P_1 + B_2 - N(\gamma_1 + k\gamma_2) \\
N_{xx}^0 &= N, \quad N_{yy}^0 = kN
\end{aligned} \tag{11}$$

— In-phase vibration

In the case of in-phase vibration, two graphene sheets vibrate synchronously and it means that there is no relative displacement between them $(w_1 = w_2)$. The equation (12) represent the vibrational frequency for in-phase vibration

$$\omega_{in} = \sqrt{\frac{-A_2 + \sqrt{A_2^2 - 4A_1A_3}}{2A_1}} \tag{12}$$

where

$$\begin{aligned}
A_4 &= \rho h(\gamma_4 - \mu^2\delta_1)(B_3 - B_2) + \frac{\rho h^3}{12}(\delta_1 - \mu^2\delta_2)P_3 \\
A_5 &= P_3(B_3 - B_2) - B_2(B_4 - B_2)
\end{aligned} \tag{13}$$

5. NUMERICAL RESULTS AND DISCUSSIONS

The material and geometrical properties of the orthotropic graphene sheet are adopted from papers [12,21] as follows: Young's modulus $E_1 = 1130\,GPa$ and $E_2 = 1050\,GPa$ of the orthotropic graphene sheet, mass density $\rho = 2250 kg/m^3$, Poisson's ratio $\nu_{12} = 0.112$ and $\nu_{21} = 0.0803$, shear modulus $G_{12} = E_1 / 2(1+\nu_{12}) = 508.09\,GPa$ and $G_{13} = G_{23} = \frac{5}{6}G_{12} = 423.41 GPa$, thickness of graphene sheet $h = 0.34\,nm$. In the present study we have used the value for the magnetic field strength in the range $H_x = 0 \div 0.1251 A/nm$ and in the case of a square nanoplate with the dimensions $10\,nm$ it corresponds to the value of dimensionless magnetic parameter ($MP = \eta h H_x^2 \, a^2 / D_{11}$) within the limits $0 \div 180$. Also, we have used the values $k_0 = 0.15\ GPa/nm$, $k_w = 0.075\ GPa/nm$, $k_G = 0.75\ N/m$, as in Ref. [12]. In the comparison study the following dimensionless parameters are used:

$$\omega_{N1} = \omega^2 a^2 \sqrt{\frac{\rho h}{D_{11}}},\ \omega_{N2} = \frac{\omega^2 a^2}{\pi^2}\sqrt{\frac{\rho h}{D_{11}}},\ k_{wN} = \frac{k_w a^4}{D_{11}},$$

$$k_{GN} = \frac{k_G a^2}{D_{11}},\ k_{0N} = \frac{k_0 a^4}{D_{11}}, MP = \frac{\eta h H_x^2 a^2}{D_{11}}$$

— Parametric study

In this section, the effects of magnetic field strength, in-plane preload (compression and tension), various boundary conditions and size of nanoplate on the vibrational behaviour of DLGSs are discussed in detail.

Figure 2(a) and (b) shows the variations of in-phase frequency with respect in-plane (uniaxial and biaxial) compression preload and various boundary conditions. The value of magnetic field strength is H_x=0.05 A/nm. In the case of uniaxial compression, the value of the frequency has the fastest decrease in the case of CSCS boundary conditions, and the slowest one in the case of SCSC boundary conditions.

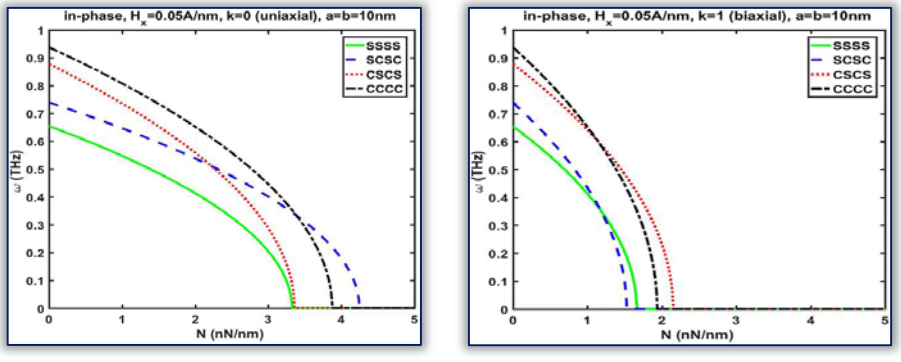

(a) (b)

Figure 2. Change in in-phase frequency with respect to compression preload (uniaxial, biaxial) and various boundary conditions for magnetic field strength H_x=0.05 A/nm ($\mu = 1.345\,nm$)

In the case of biaxial compression shown in Figure 2b the value of the frequency has the fastest decrease in the case of CCCC boundary conditions, and the slowest one in the case of SSSS boundary conditions.
In relation to Fig 2 (a) and (b), in Fig 3 (a) and (b) only the value of magnetic field strength has been increased to H_x=0.1 A/nm. All the other parameters have the same value. A significant influence of magnetic field on the vibrational behaviour of DLGS can be seen. In both cases of (uniaxial and biaxial) compression the value of the frequency has a faster decrease in the case of CCCC and SCSC boundary conditions.

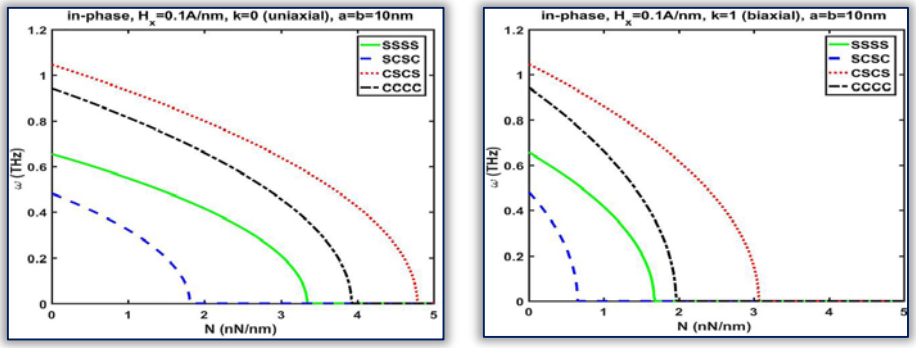

(a) (b)

Figure 3. Change in in-phase frequency with respect to compression preload (uniaxial, biaxial) and various boundary conditions for magnetic field strength H_x=0.1 A/nm ($\mu = 1.345\,nm$)

From Figure 4 (a) and (b) it can be clearly seen that in the case of out-of-phase vibration the value of the frequency for the case of CCCC and CSCS boundary conditions decreases significantly faster with the increase of value of in-plane preload (for uniaxial compression) in relation to the case of in-phase vibration. For biaxial compression, it can be noticed from Figure 4b that the value of the frequency has the slowest decrease for the case of SSSS boundary conditions, and the fastest one for the case of CCCC boundary conditions.

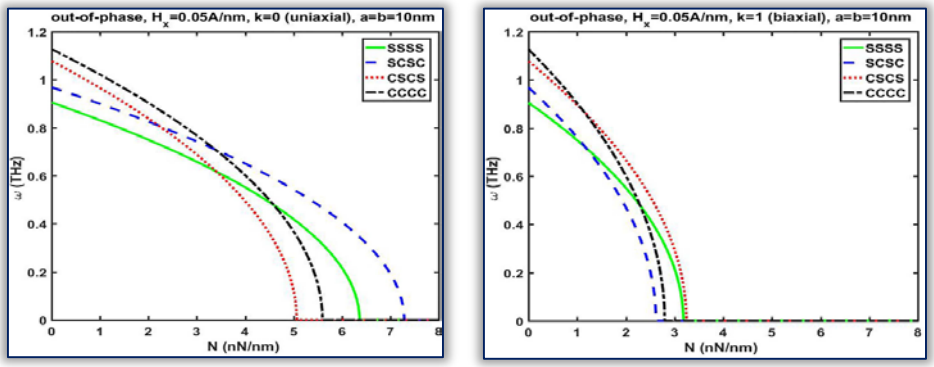

(a) (b)

Figure 4. Change in out-of-phase frequency with respect to compression preload (uniaxial, biaxial) and various boundary conditions for magnetic field strength H_x=0.05 A/nm ($\mu = 1.345\,nm$)

At the value of magnetic field strength Hx=0.1 A/nm in the case of out-of-phase vibration from Figure 5(a) and (b) it can be noticed that the value of the frequency for the case of CCCC boundary conditions decreases significantly faster in relation to other three cases of boundary conditions.

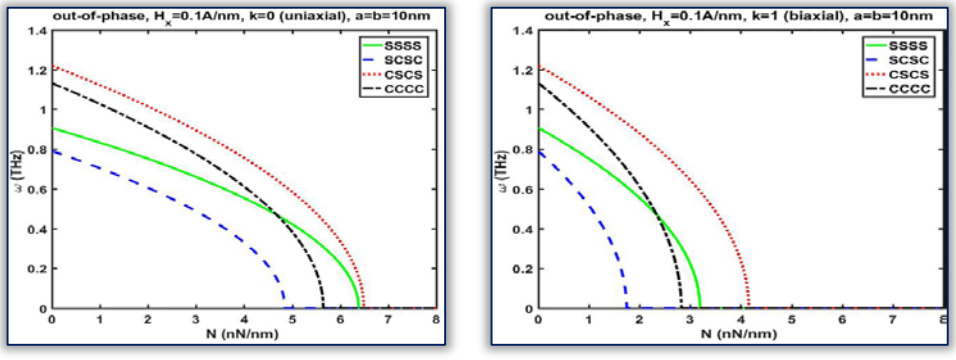

(a) (b)

Figure 5. Change in out-of-phase frequency with respect to compression preload (uniaxial, biaxial) and various boundary conditions for magnetic field strength H_x=0.1 A/nm ($\mu = 1.345\,nm$)

The effects of increasing the magnetic field strength on the in-phase frequency of rectangular DLGS (a=10nm, b=15nm) with different boundary conditions are investigated in Figure 6 (a) and (b). In Figure 6a DLGS is loaded with uniaxial

compression force N=2 nN/nm, and in Figure 6b with uniaxial tension force N=10 nN/nm. With the increase of value of the magnetic field strength the value of the frequency increases for all four cases of boundary conditions. The value of the in-phase frequency in the case of uniaxial compression has the fastest increase in the case of CSCS boundary conditions and the slowest one in the case of SCSC boundary conditions. In the case of uniaxial tension (N=10 nN/nm) shown in Figure 6b the value of in-phase frequency for CCCC and CSCSC boundary conditions is very close. It is the same with SSSS and SCSCS boundary conditions. In the case of activity of uniaxial tension force, the value of the in-phase frequency increases proportionally for all four observed cases of boundary conditions.

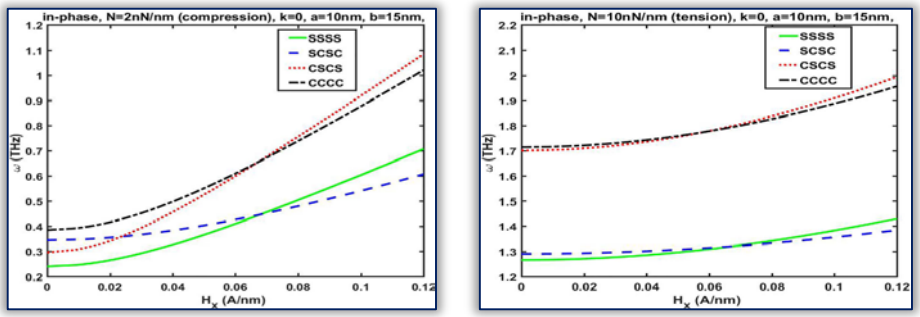

(a) (b)

Figure 6. Change in in-phase frequency with respect to magnetic field strength, various boundary conditions and uniaxial in-plane (compression and tension) preload ($\mu = 1.345\,nm$)

Figure 7 (a) and (b) represents the effects of the magnetic field strength and various boundary conditions on out-of-phase frequency for rectangular DLGS (a=10 nm, b=15 nm). In Figure 7a DLGS is exposed to the activity of uniaxial compression force (N=4 nN/nm), and in Figure 7b to the activity of uniaxial tension force (N=4 nN/nm). It is obvious from Figure 7a that in the case of activity of uniaxial compression force with the increase of value of the magnetic field strength the value of the out-of-phase frequency has the fastest increase in the case of CSCS boundary conditions. From Figure 7b it can be noticed that the activity of uniaxial tension force in the case of out-of-phase vibrations causes the same effect as in the case of in-phase vibrations shown in Figure 6b.

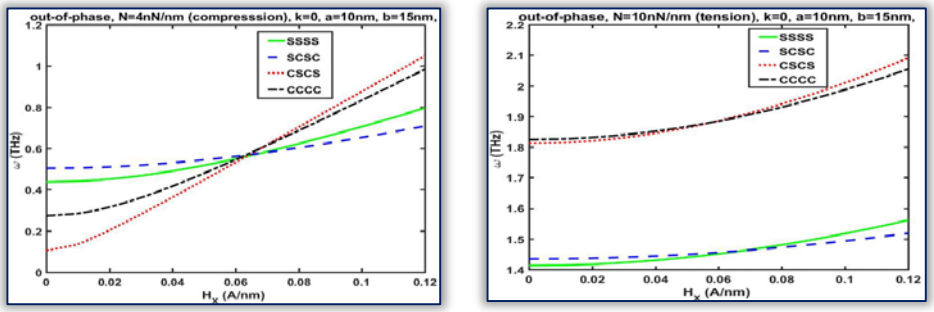

(a) (b)

Figure 7. Change in out-of-phase frequency with respect to magnetic field strength, various boundary conditions and uniaxial in-plane (compression and tension) preload ($\mu = 1.345\,nm$)

Figs. 8, 9, 10 and 11 illustrate the effect of the size of the graphene sheet and increasing of the magnetic field strength on the in-phase frequency for SSSS, CCCC, SCSC and CSCS boundary conditions respectively. In Figure 8a, 9a, 10a, 11a DLGS is exposed to the activity of biaxial compression force, and in Fig 8b, 9b, 10b, 11b to the activity of biaxial tension force.

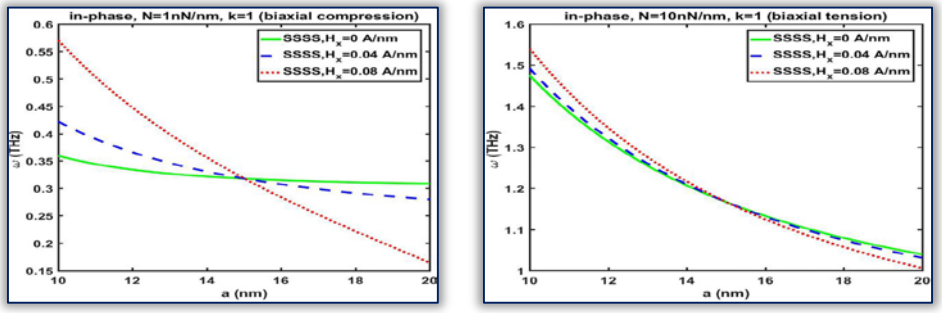

(a) (b)

Figure 8. Change in in-phase frequency with respect to length of DLGS, magnetic field strength and biaxial in-plane (compression and tension) preload for SSSS boundary conditions ($\mu = 1.345\,nm$)

It can be concluded from Figure 8 and Figure 9 that in the case of square nanoplates $(a = b = 15\,nm)$, the change of magnetic field strength value under SSSS and CCCC boundary conditions does not affect the in-phase frequency value.

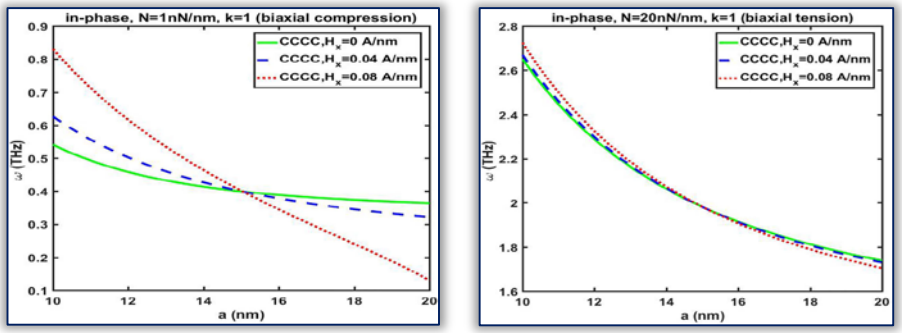

(a) (b)

Figure 9. Change in in-phase frequency with respect to length of DLGS, magnetic field strength and biaxial in-plane (compression and tension) preload for CCCC boundary conditions ($\mu = 1.345\,nm$)

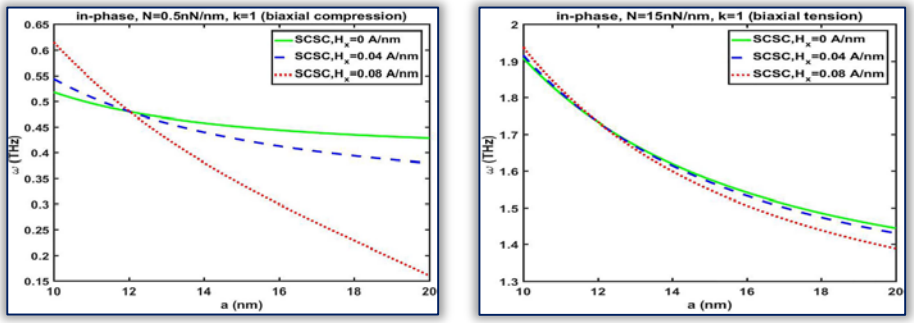

(a) (b)

Figure 10. Change in in-phase frequency with respect to length of DLGS, magnetic field strength and biaxial in-plane (compression and tension) preload for SCSC boundary conditions ($\mu = 1.345\,nm$)

It can be seen from Figure 10 that, in the case of rectangular nanoplates $(a \approx 12\,nm,\ b = 15\,nm)$, the change of magnetic field strength value under SCSC boundary condition does not affect the in-phase frequency value.

Finally, from Figure 11 it can be noticed that in case of rectangular nanoplates $(a \approx 18\,nm,\ b = 15\,nm)$, the change of magnetic field strength value under CSCS boundary condition does not affect the in-phase frequency value.

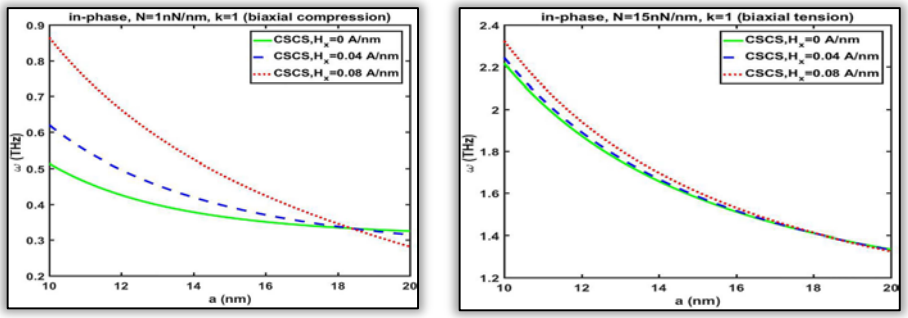

(a) (b)

Figure 11. Change in in-phase frequency with respect to length of DLGS, magnetic field strength and biaxial in-plane (compression and tension) preload for CSCS boundary conditions ($\mu = 1.345\,nm$)

These three cases, when the value of the in-phase frequency is independent from the change of value of the magnetic field strength at certain dimensions of DLGS occur in the case of biaxial compression and biaxial tension.

6. CONCLUSION

In this paper, by using Hamilton's principle, the equations of motion and boundary conditions were obtained base on the new first order shear deformation theory in the framework of the Eringen's differential nonlocal elastic law. The Galerkin's method has been used to solve the equations of motion of the DLGS for SSSS, CCCC, CSCS and SCSC boundary conditions. Numerical results are presented to investigate the effects magnetic field strength, initial preload (compression and tension), size of nanoplate and boundary conditions on vibrational frequency. It is observed that increasing the in-plane compression preload degrades the graphene sheet stiffness and frequency reduce until a critical point in which frequency becomes zero. Also, the frequency increase with the increase of the magnetic field strength for rectangular DLGS $(a = 10\,nm,\ b = 15\,nm)$.

Note: This paper is based on the paper presented at COMETa 2018 – The 4th International Conference on Mechanical Engineering Technologies and Applications, organized by Faculty of Mechanical Engineering, University of East Sarajevo, in Jahorina, BOSNIA & HERZEGOVINA, in 27–30 November, 2018.

References

[1] Eringen, AC., Edelen, DGB. (1972). On nonlocal elasticity. International Journal of Engineering Science, 10, p.p. 233-248.
[2] Eringen, AC. (1983). On differential equations of nonlocal elasticity and solutions of screw dislocation and surface waves. Journal of Applied Physics, 54, p.p. 4703-4710.
[3] Reddy, JN. (2007). Nonlocal theories for bending, buckling and vibrations of beam. International Journal of Engineering Science, 45, p.p. 288-307.
[4] Pradhan, SC., Phadikar, JK. (2009). Nonlocal elasticity theory for vibration of nanoplates. Journal of Sound and Vibration, 325, p.p. 206-223.
[5] Mindlin, R. (1965). Second gradient of strain and surface-tension in linear elasticity. International Journal of Solides and Structures, 1, p.p. 414-438.
[6] Kong, S., Zhou, S., Nie, Z., Wang, K. (2009). Static and dynamic analysis of micro beams based on strain gradient elasticity theory. International Journal of Engineering Science, 47, p.p. 487-498.
[7] Koiter, WT. (1964). Couple- stress in the theory of elasticity: I and II. Royal Netherlands Academy of Arts and Sciences, 67, p.p. 17-44.
[8] Agköz, B., Civalek, Ö. (2012). Free vibration analysis for single-layered graphene sheets in an elastic matrix via modified couple stress theory. Materials and Design, 42, p.p. 164-171.
[9] Murmu, T., Pradhan, SC. (2009). Vibration analysis of nanoplates unde uniaxial prestressed conditions via nonlocal elasticity. Journal of Applied Physics, 106, 104301.
[10] Kiani, K. (2012). Vibration analysis of elastically restrained double-walled carbon nanotubes on elastic foundation subjected to axial load using nonlocal shear deformable theories. International Journal of Mechanical Sciences, 68, p.p. 16-34.
[11] Mohammadi, M., Goodarzi, M., Ghayour, M., Farajpour, A. (2013). Influence of in-plane pre-load on the vibration frequency of circular graphene sheet via nonlocal continuum theory. Composites Part B, 51, p.p. 121-129.
[12] Radić, N., Jeremić, D. (2017). A comprehensive study on vibration and buckling of orthotropic double-layered graphene sheets under hygrothermal loading with different boundary conditions. Composites Part B, 128, p.p. 182-199.
[13] Güven, U. (2014). Transverse vibrations of single-walled carbon nanotubes with initial stress under magnetic field. Composite Structures, 114, p.p. 92-98.
[14] Murmu, T., McCarthy, MA., Adhikari, S. (2012). Vibration response of double-walled carbon nanotubes subjected to an externally applied longitudinal magnetic field: A nonlocal elasticity approach. Journal of Sound and Vibration, 331, p.p. 5069-5086.
[15] Kiani, K. (2014). Vibration and instability of a single-walled carbon nanotube in a three-dimensional magnetic field. Journal of Physics and Chemistry of Solids, 75, p.p. 15-22.
[16] Murmu, T., McCarthy, MA., Adhikari, S. (2013). In-plane magnetic fields affected transverse vibration of embedded single-layer graphene sheets using equivalent nonlocal elasticity approach. Composite Structures, 96, p.p. 57-63.
[17] Kiani, K. (2014). Free vibration of conducting nanoplates exposed to unidirectional in-plane magnetic fields using nonlocal shear deformable plate theories. Physica E, 57, p.p. 179-192.
[18] Ghorbanpour, Arani AH., Maboudi, MJ., Ghorbanpour, Arani A., Amir, S. (2013). 2D Magnetic field and biaxial in-plane pre-load effects on the vibration on double bonded orthotropic graphene sheets. Journal of Solids Mechanics, 5, p.p. 193-205.
[19] Karličić, D., Cajić, M., Adhikari, S., Kozić, P., Murmu, T. (2017). Vibrating nonlocal multi-nanoplate system under inplane magnetic field. European Journal of Mechanics A/Solids, 64, p.p. 29-45.
[20] Radić, N., Jeremić, D., Mijatović. B. (2018). Vibration analysis of orthotropic double-nanoplate system subjected to unidirectional in-plane magnetic field with various boundary conditions, IOSR Journal of Mechanical and Civil Engineering (IOSR-JMCE), Volume 15, Issue 3, Ver. IV, p.p 59-76.
[21] Ni, Z., Bu, H., Zou, M., Yi, H., Bi, K., Chen, Y. (2010). Anisotropic mechanical properties of graphene sheets from molecular dynamics. Physica B, 405, p.p. 1301-1306.

ISSN 1584 - 2665 (printed version); ISSN 2601 - 2332 (online); ISSN-L 1584 - 2665